*Journal of the Korean Nuclear Society*
*Volume 5, Number 4, December, 1973*

≪Original≫

# Dosimetrical Analysis of Reactor Leakage Gamma-rays by Means of Scintillation Spectrometry

Jae Shik Jun

Korea Atomic Energy Research Institute, Seoul, Korea

(Received July 12, 1973)

## Abstract

Exposure rates due to leakage gamma-rays from operating reactors TRIGA Mark II and III were measured in a horizontal plane by means of scintillation spectrometry using a 3″×3″ cylindrical NaI(Tl) detector associated with a 400 channel pulse height analyzer under varied conditions of reactor operation.

In determining exposure rate due to the leakage gamma-rays at each point of measurement, Moriuchi's spectrum-exposure rate conversion theory was applied instead of using conventional responce matrix method which necessitates very complicated procedures to convert a spectrum into exposure rate.

The results show that a basic pattern of "typical" spectrum of the reactor leakage gamma-rays is neither affected by thermal output of the reactor, nor influenced by overall attenuation in radiation intensity. It was indicated that the attenuation of the leakage gamma-rays in air in terms of exposure rate as a whole follows an exponential law, and the total exposure rate due to the leakage gamma-rays at a certain point is nearly proportional to thermal output of the reactor. The complexity in spectrum measured for a movable core reactor, TRIGA Mark III, was analyzed through spectrum resolution, and proper judgement of the leakage gamma-rays in a complex spectrum was discussed.

## 요 약

TRIGA Mark Ⅱ와 Ⅲ 原子爐의 여러가지 稼動條件에 있어서 爐壁으로 부터의 漏洩 γ線에 依한 照射線量率을 3″×3″ 圓筒型 NaI(Tl) 閃光計數器와 400 channel 波高分析裝置로 測定 하였는데 測定된 spectrum으로 부터 照射線量率을 算出하는데는 實際的面에서 복잡하기 짝이 없는 respense matrix 方法대신 精度가 좋으면서도 比較的 그 과정이 단순한 Moriuchi의 spectrum 一照射線量率 換算 理論을 적용하였다.

硏究結果에 따르면 爐心에서 發生된 漏洩 γ線의 基本的인 spectrum 형태는 原子爐의 熱出力이나 遮蔽壁에 依한 强度의 減衰에 별로 영향을 받지 않고 있으며 原子爐 漏洩γ線에 의한 全照射線量率의 空氣中에서의 減衰는 幅 넓은 energy 分布에도 不拘하고 指數函數的 減衰를 하고 있음이 判明되었다. 이 全照射線量率은 原子爐의 熱出力에 대체로 比例하고 있으나 TRIGA Mark Ⅲ과 같은 可動型爐心의 경우는 測定된 spectrum이 매우 多樣한바, 그로부터 算出된 全照射線量率의 크기에는 관계없이. spectrum 分解方法을 적용하여 爐心에서 發生된 漏洩 γ線과 原子爐稼動中 發生되는 餘地 γ線의 寄與를 判別 解釋하는데 成功하였다.

## 1. Introduction

Leakage gamma-rays from a reactor shielding wall become one of the important gamma-ray sources in the reactor hall during the course of reactor operation. Hence, the quantitative analysis of the leakage gamma-rays are very important both in health physics and in nuclear engineering point of view.

Few publications, however, have so far dealt with leakage gamma-rays in the outside of the reactor wall, although there are several papers concerned with the in-core gamma-ray spectrometry[1-5]. A study on reactor leakage gamma-rays was carried out by Nakashima *et al.*,[6] but their interests were limited to several locations in a fixed-core reactor hall, and for conversion of the measured spectra to exposure rate they used conventional response matrix method which is too complicated to be applied conveniently in practical situations.

In this work, the leakage gamma-rays out of the reactors TRIGA Mark II and III were studied, in a radial plan crossing the core center, by means of scintillation spectrometry. The measured spectra were directly converted into exposure rate in accordance with the "spectrum-exposure rate conversion operation"[7-9] instead of applying the response matrix method which involves the solution of a number of simultaneous equations and accordingly necessitates a computer to solve the constructed matrix equations.

The reactor TRIGA Mark II is a pool type reactor with a fixed core, while TRIGA Mark III is pool type reactor of a movable core. The spectra of the leakage gamma-rays were measured at different thermal output of the reactors, and measured for different core positions in the case of TRIGA Mark III.

All the spectra measured were converted into exposure rate and the leakage gamma-rays are presented in terms of $\mu$R/hr. At the same time, investigations on the gamma-rays other than the leakage gamma-rays originating during the reactor operation were carried out on the basis of spectrum analysis. Overall pattern of the attenuation of the reactor leakage gamma-rays in air were also examined in terms of exposure rates as a whole.

## 2. Spectrometry

### 1) Instruments

As is well known, the gamma-rays originating in core during the reactor operation are classified as[5]; (1) prompt gamma-radiations from $^{235}U$ fission, (2) fission product gamma-rays, (3) gamma-rays from radiative capture $(n, \gamma)$ reactions, (4) gamma-rays from inelastic scattering of nentrons, and (5) activation products gamma-rays. The energies of those gamma photons ranges widely from a few KeV to around 10 MeV. but the relative contribution of the photons with energies higher than 7.5 MeV are negligible in practice[1-3, 10]. Therefore, the range of the energies of leakage gamma-rays is expected to be in the similar region, althrough there must be sufficient attenuation occured during the passages of the photons through shielding wall.

Since conventional health physics survey instruments are not suitable to measure photons of such an energy that covers so wide a range because of unknown energy dependence of the instruments, gamma-ray scintillation spectrometry was applied to determine the exposure rate due to the leakage gamma-rays with good accuracy.

For the spectrometry of the leakage gamma-rays a $3'' \times 3''$ cylindrical NaI(Tl) scintillation detector, which holds good linearity between the incident photon energy and output pulse height, was used with a 400 channel pulse height analyzer. In the light of the expected energy range of the leakage gamma-rays, the measurable range of the spectrome-

ter was adjusted so as to detect incident photons of energies upto 10 MeV. However, because of inherent limitation in the lowest effective channels of the pulse height analyzer (7~8 channels for 400-channel operation) the minimum detectable energy was limited to 0.1 MeV in this investigation.

The detector probe was shielded around with lead of 5 cm in thickness to reduce the contribution of natural beckground radiation to as little as possible. An estimation shows that the lead of this thickness is able to make a broad beam of 1~2 MeV photons attenuate to a fraction of 0.06~0.1, and for 0.4~0.7 MeV photon beam it attenuates the intensity down to a fraction of $10^{-4}$~$10^{-3}$ [11].

Height of the detector was maintained at 1 m above the floor of the reactor hall to make it nearly coincident with the horizontal center line of the reactor cores and also with the average body height of the working personnel. The detector was arranged to contact vertically with the reactor wall surface without collimation. The whole arrangement for leakage gamma-ray spectrometry is shown in Fig. 1.

Linearity between the incident photon energy and output pulse height of the spetrometer was periodically checked during the course of spectrometry using standard gamma-ray sources such as $^{133}$Ba(0.356 MeV), $^{137}$Cs (0.662 MeV), $^{60}$Co(1.173 MeV, 1.332 MeV and 2.505 MeV sum peak) and $^{88}$Y(0.898 MeV, 1.836 MeV and 2.734 MeV). As shown in Fig. 2, slight non-linearity was observed in the region of energy lower than 1.5MeV and corrections for this effect was made prior to analyzing each leakage gamma-ray spectrum. The relatioship between the output pulse height from the spectrometer per unit energy versus energy of the incident photon is also shown in Fig. 2. This effect of non-linearity in low energy region is explained as the result of a variation of the fluorescence efficiency of NaI(Tl) crystal with gamma energy in this region[12].

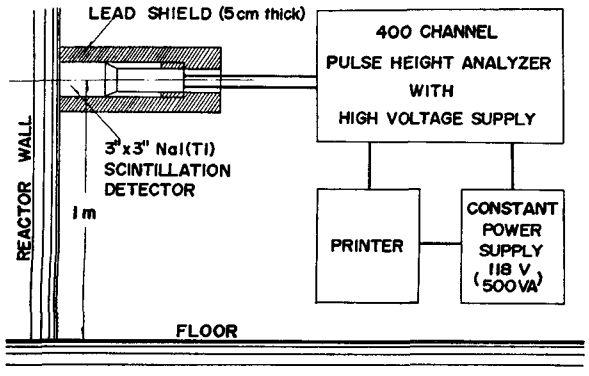


**Fig. 1. Experimental layout for reactor leakage gamma-ray spectrometry.**

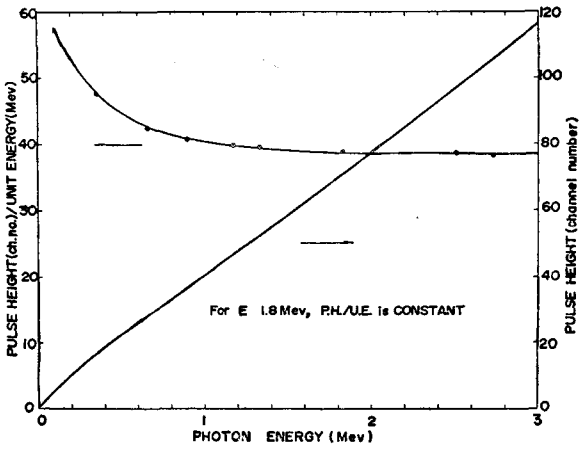


**Fig. 2. Observed non-leanear relationship, in NaI(Tl) detector, between output pulse height and incident photon energy in low energy region**

### 2) Condition of the Measurements

The TRIGA Mark II is a fixed-core swimming pool type reactor which was originally designed to operate at 100KW thermal output and in 1969 the operating power was upgraded to 250KW with the shield remaining unaltered. TRIGA Mark III, on the other hand, is a swimming pool type reactor with a movable

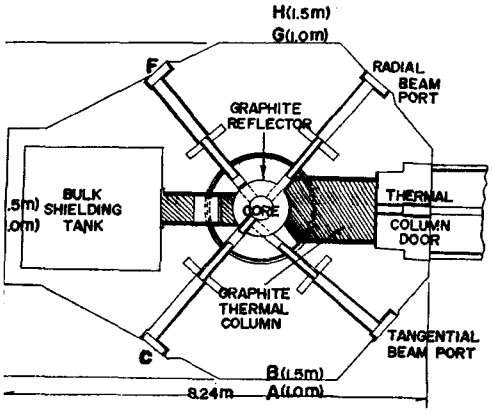


Fig. 3. Horizontal section of reactor TRIGA Mark II.

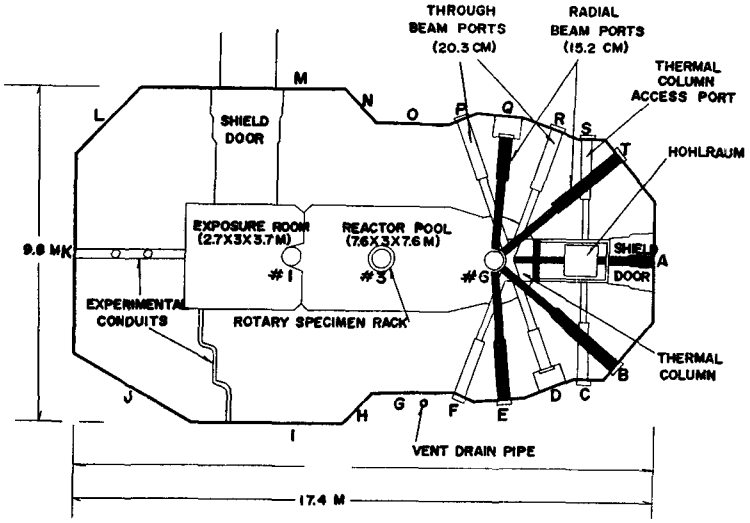


Fig. 4. Horizontal section of reactor TRIGA Mark III.

Table 1. Conditions of reactor leakage gamma-ray spectrometry

| Reactor | Thermal Output | Core Position | Point of Measurement |
|---|---|---|---|
| TRIGA II | 100KW | — | A, D, G(at 0, 50, 100 cm from wall surface) |
| | 250KW | — | A, D, G ( 〃 〃 ) |
| TRIGA III | 1MW | #1 | A**, B, D*, E, F*, G, I, K, M, O, P*, T, vdp. |
| | 〃 | #3 | A**, B, D*, E, F*, G, I, K, M, O, P*, R*, T, vdp. |
| | 〃 | #6 | A**, B, D*, E, F*, G, I, K, M, O, P*, R*, T, vdp. |
| | 2MW | #3 | A**, B, D*, E, F*, G, I, K, M, O, P*, T, vdp. |
| | 〃 | #6 | A**, D*, E, F*, G, I, K, M, O, P*, T, vdp. |

*; at 15 cm from the wall surface
**; at 45 cm from the wall surface

core and the maximum thermal output is available at 2 MW except for the core position at biological irradiation cell.

Therefore, the spectra of the leakage gamma-rays were measured for TRIGA Mark II at 100 and 250 KW thermal outputs, while for TRIGA Mark III, they were measured on 1 and 2 MW operations with three different core positions, namely, core positions #1(biological irradiation position), #3 (isotope production position), and #6 (physics experiment position). However, 2MW operation at core position #1 was avoided because of the possible release of a large amount of activated gases such as $^{41}Ar$ from the irradiation cell.

The points of the measurements were labeled alphabetically as shown in Figs. 3 and 4, and the condition of the leakage gamma-ray spectrometry are summarized in Table 1.

In the case of TRIGA Mark II, three positions of typical shielding wall, which do not involve any experimental facilities such as beam ports or thermal column, were selected to investigate typical pattern of the leakage gamma-ray spectrum at point of 1 m height above the ground floor, *i.e.*, A, D and G points (B, E and H points are 1.5 m height on the same walls, respectively. -refer to Fig. 3). The effect of distance on the exposure rates due to the leakage gamma-rays were also exa-

mined in the region of 1 m distant from the reactor wall surface where personnel are most probably staying at work.

For TRIGA Mark III, on the contrary, the measurements were carried out for most parts of the walls since the patterns of the spectra were expected to be varied depending on the operating core positions. As it was just after the reactor start-up, all the beam ports and thermal columns had been remained closed during the course of the spectrometry. At some points of the measurements, however, it was not able to contact the detector to the reactor wall surface because of protruded things such as beam port plugs or accessary facilities. But the values of the exposure rate as a whole at those wall surfaces might be numerically deduced from the attenuation pattern observed in the case of TRIGA Mark II as far as the leakage gamma-rays are concerned.

## 3. Spectrum-Exposure Rate Conversion

### 1) Theoretical Background

In order to determine exposure rate from a gamma-ray spectrum obtained by scintillation spectrometry, response matrix method has been generally used[6, 13-16]. This method is, however, so complicated that it is almost not useful in practical situation of radiation protection work, since the method involves such tedious processes as; construction of response matrix under a certain condition using standards spectra of various energies covering the enitre necessary energy range in reasonable energy bins, inversion of the matrix which necessitates a computer work, calculation of incident photon fluence as function of energy, and conversion of the photon fluence spectrum into the exposure rate. In the particular situation of determiming the exposure rate due to reactor leakage gamma-rays at a number of points, the work to be carried out for converting the spectra into exposure rates is not simple, and the necessary energy range to be covered is upto 10 MeV, hence the application of the response matrix method is impractrical not only in economical point of view, but also in obtaining standards spectra to cover so wide a range of energy.

Recently, however, Moriuchi and Miyanaga carried out a series of work on the direct conversion of measured gamma-ray spectrum into exposure rate with satisfatory accuracy by introducing an appropriate conversion operator[7-9]. Background of the theory can briefly be summarized as follows.

When a gamma-ray spectrum is obtained by a scintillation spectrometer, it is assumed that the output pulse height from the photomultiplier is linearly proportional to the energy of secondary electrons generated by photoelectric absorption or Compton scattering or pair production process of the incident photons in the NaI(Tl) crystal.

Let the pulse height distribution of the secondary electron of energy $E$(MeV) due to the incident photon of energy $E_0$(MeV) of unit flux density (photons/cm$^2$ sec) be $f(E, E_0)$. And let the exposure rate in the identical gamma-ray field be $D(E_0)$.

If there exists a function $G(E)$ to satisfy the integral equation

$$D(E_0)=\int_0^{\infty} f(E, E_0)\ G(E)dE \qquad (1)$$

for photons of any energy, $E_0$, in arbitry energy interval, it is possible to obtain the exposure rate of the field directly from the measured spectrum. Here, $G(E)$ is so-called appearent spectrumexposure rate conversion operater and it makes the NaI(Tl) scintillator free from energy dependence in the estimation of the exposure rate. The existence of the $G(E)$ function for NaI(Tl) crystal and incident photons has been thoroughly examined by

Miyanage and Moriuchi[8].

In a complex field of gamma photons of various energies the measured spectrum $F(E)$ is written as

$$F(E)=\sum_j \phi(E_j)\ f(E,E_j) \qquad (2)$$

where $\phi(E_j)$ is the incident photon flux of energy $E_j$ MeV. Since Eq. (1) is assumed to be satisfied for photons of any energy,

$$D(E_j)=\int_0^{\infty} f(E,E_j)\ G(E)dE$$

comes also into existence.

Then, the total exposure rate, $D$, due to the photons of complex energy in the field is given by

$$\begin{aligned} D&=\sum_j \phi(E_j)\ D(E_j)\\ &=\sum_j \int_0^{\infty} \phi(E_j)\ f(E,E_j)\ G(E)dE\\ &=\int_0^{\infty} F(E)\ G(E)dE \end{aligned} \qquad (3)$$

Therefore, the total exposure rate in a given gamma-ray field is easily determined from the measured spectrum, $F(E)$, if the value of $G(E)$ is known.

**2) Calculation of $G(E)$**

In the latest work of Moriuchi[9], he calculated numerical values of $G(E)$ function for several NaI(Tl) crystals of different sizes by means of polynomial curve fittings to the experimentally obtained standard spectra with an aid of computer calculations. For this procedure, however, plenty standard sources of various energies to cover the entire range of interest are necessary, and yet there remain some technical matters of choosing proper limit of approximation or handling the "edge effect" of the $G(E)$ values, etc. As an alternative mode, amanual calculation of $G(E)$ values is possible when the spectrum is modelized to consist of mainly two parts, *i.e.*, photolectric peak and Compton continuum including some escape peaks due to pair production in higher energy region. The energy region to be integrated in numerical calculation of $G(E)$ is limited from the mininum practically significant energy to the maximum energy of incident photons. Under this condition, Eq. (1) is written as

$$\begin{aligned} D(E_0)&=\int_{E\min}^{E_0} f(E,E_0)\ G(E)dE\\ &=f(E_0,E_0)\ G(E_0)+\int_{E\min}^{E_c} f(E,E_0)\ G(E)dE\\ &=I(E_0)P(E_0)G(E_0)+\int_{E\min}^{E_c} f(E,E_0)\,G(E)dE \end{aligned} \qquad (4)$$

where $E_0$ : incident photon energy (MeV)

$E_c$ : Compton edge energy (MeV)

$E_{\min}$ ; minimum practically significant energy (MeV)

$I(E_0)$: interaction ratio of NaI (Tl) scintillator for incident photons of energy $E_0$

$P(E_0)$: photofraction of NaI(Tl) scintillator for incident photons of energy $E_0$.

From Eq. (4), $G(E_0)$ becomes

$$\begin{aligned} G(E_0)=&\frac{D(E_0)}{I(E_0)P(E_0)}\\ &-\frac{1}{I(E_0)P(E_0)}\int_{E\min}^{E_c} f(E,E_0)\ G(E)dE \end{aligned} \qquad (5)$$

If pulse height distribution in the Compton continuum is assumed to be uniform in the energy interval from 0 to $E_c$ (this assumption causes no significant error in the energy range considered here for a crystal as large as $3''\times3''$ [8]), the spectrum in the region may be written as

$$F(E,E_0)=I(E_0)\ [1-P(E_0)]/E_c,\quad E\leq E_c \qquad (6)$$

Substituting Eq. (6) into Eq. (5), we obtain

$$\begin{aligned} G(E_0)=&\frac{D(E_0)}{I(E_0)P(E_0)}\\ &-\frac{1-P(E_c)}{E_c\ P(E_0)}\int_{E\min}^{E_c} G(E)dE \end{aligned} \qquad (7)$$

As mentioned earlier, $D(E_0)$ is the exposure rate in a field of gamma-rays of energy $E_0$ of unit flux density, and thus, is simply determined by

$$D(E_0)=65,664\ E_0\left(\frac{\mu_a}{\rho}\right)_a (\mu\text{R/hr per}$$

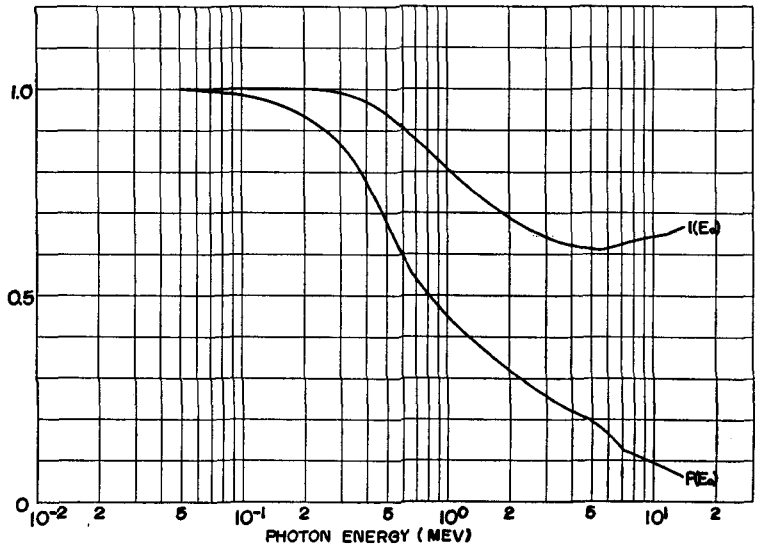


**Fig. 5. Interaction ratio ($I(E_0)$) & photofraction ($P(E_0)$) of 3″×3″ NaI (Tl) scintillator for broad parallel beam of incident photons (after ref. 18)**

photons/cm² sec)
in accodance with the relationship between photon flux and exposure rate[17]. Here, $(\mu_a/\rho)_a$ is true mass absorption coefficient of air.

Since a spectrum of gamma-rays of energy less than 0.1~0.15MeV is mainly constituted of photofraction, $G(E)$ values are easily calculated dropping the second term of Eq. (7) when $E_{min}$ exists in this low energy region. And since $E_0$ is always larger than $E_c$ in higher energy region, the values of $G(E)$ can be calculated by Eq. (7) in sequence from the determined values of $G(E)$ at lower energies.

For actual calculation of numerical values of $G(E)$, the energy region of 0.05 to 10 MeV was divided into 63 intervals. They were calculated at 10 KeV intervals in 0.05 to 0.1 MeV region, at 50 KeV intervals in 0.1 to 1 MeV region, and at 200 KeV intervals in 1 to 10 MeV region, resprectively. Miller-Snow's values[18] of $I(E_0)$ and $P(E_0)$ which were calculated theoretically for a broad parallel beam incident vertically on the front surface of 3″×3″ cylindrical NaI(Tl) crystal were applied in the $G(E)$ value determination. Fig. 5 shows the values of $I(E_0)$ and $P(E_0)$ as functions of

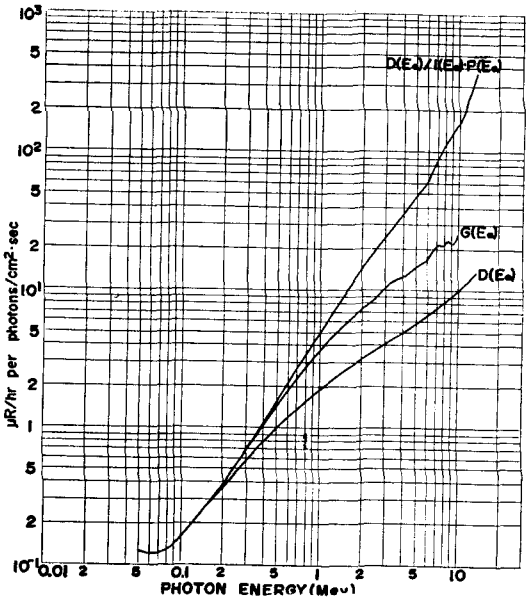


**Fig. 6. $D(E_0)$, $D(E_0)/I(E_0)$ $P(E_0)$ & $G(E_0)$ for 3″×3″ NaI(Tl) scintillation detector.**

incident photon energy.

Angular dependence of the exposure rate estimated by this method is known to be less than ±5%[7] when the angles of incident photons to the crystal axis are smaller than 90°. As shown in Fig. 1, this condition was geometrically satisfied throughout the spectrometry of the reactor leakage gamma-rays.

Calculated values of $D(E_0)$, $D(E_0)/I(E_0)$

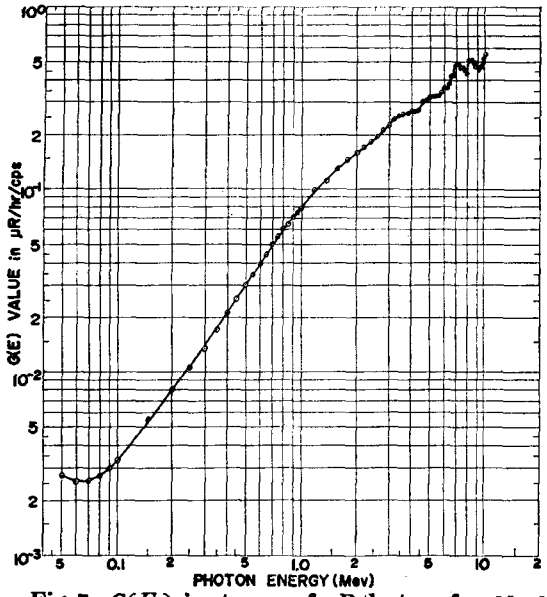


**Fig. 7. $G(E_0)$ in terms of μR/hr/cps for 3″×3″ NaI(Tl) scintillation detector**

$P(E_0)$ and $G(E_0)$ expressed in terms of exposure rate per unit photon flux density are shown in Fig. 6 as functions of photon energy. In calculating $D(E_0)$, Evans' values of true mass absorption coefficient of air[19] were applied.

Fig. 6 shows that the values of three quantities are well coincident with each other in low energy region (<0.2MeV) where photoelectric process is the main cause of photon absorption in the crystal, while the higher the energy of incident photon becomes, the more widely the values split from each other due to increasing Compton portion of the absorption.

The $G(E_0)$ values were again divided by the incident surface area of the scintillation crystal (46.5 $cm^2$) in order to make direct conversion of the spectrum count rate into exposure rate possible, and the new $G(E_0)$ values are plotted in terms of μR/hr/cps as shown in Fig. 7.

This curve shows quite reasonable agreement with the curves shows in Fig. 5 of reference 9 in their tendency, although there is a slight fluctuation, in 7~10 MeV region, which seems to be tolerable as far as the conversion of the reactor leakage gamma-ray spectrum into total exposure rate is concerned.

There are two possible sorts of error may be introduced in $G(E_0)$ value calculation; one stem from modelizing the Compton continuum to be uniform, and the other comes from neglecting pair production effect in higher energy region. The fomer is known to be less than 5% in positive side for a 3″×3″ NaI(Tl) crystal and the latter is less than ±2% in the energy region of lower than 10 MeV[9]. Thus, overall error possibly introduced in $G(E_0)$ values estimated to be within ±5%.

On the other hand, the unit of exposure, R, is usually recommended to be applied for photons of energy lower than about 3 MeV[20] because of possible disturbance of secondary electron equilibrium in air due to contribution of bremsstrahlung in the volume of interest. Actually, however, since the secondary electron equilibrium coefficient of air for photon energies of 10 MeV is about 1.04 and that for 8 MeV photons which is nearly corresponding to the maximum energy in the detected leakage gamma-rays is less than 1.03[21], it is not thought to be unjustifiable to use the unit of exposure rate in terms of R per unit time in dosimetrical analysis of reactor leakage gamma-rays particularly for the primary purpose of radiation protection.

### 3) Exposure Rate Conversion

Prior to direct conversion of reactor leakage gamma-ray spectrum into exposure rate, corresponding background spectrum, which was measured under the condition of reactor shutdown, was subtracted from each measured spectrum in order to figure out the spectrum of "pure" leakage gamma-rays. Then, the energy of the net spectrum was corrected for pulse height-energy linearity as shown in Fig. 2 with the help of standard spectrum, and the values of $G(E_0)$ shown in Fig. 7 were applied

to cenvert entire spectrum into exposure rate as a whole.

Since the measured spectrum is expressed in terms of count rate per channel, the actual conversion process is to carry out summation of discret values rather than applying integral equation like Eq. (3). That is, when let the channel number be $i$, total count rate in the channel interval of energy $\Delta E$ of the spectrum be $N_i$, and corresponding $G(E)$ value of the mean energy of the channel interval be $G_i$, the total exposure rate $D$ is calculated by

$$D=\sum_{i_{min}}^{i_{max}} N_iG_i.$$

The energy resolving power of the scintillator is known to be energy dependent as a function of $E^{-\frac{1}{2}}$ [22]. Therefore, in spectrum exposure rate coversion process, the optimum ratio of channel width for giving uniform error[9] was taken into account. Thus, the total exposure rate due to the leakage gamma-rays determined by summing up individual products of the total count rate of 2 channel interval in the section between 7th and 40th channels, that of 5 channel interval in the section between 41st and 170th channels, and that of 10 channel interval in the section between 171st and 400 th channel with $G(E_0)$ values of corresponding mean energy of the channel intervals.

Standard error, $\sigma$, of the exposure rate due to counting statistics is given by

$$\sigma=\pm\frac{\sqrt{\sum N_iG_i^2/t}}{\sum N_iG_i}\times 100(\%)$$

where $t$ is counting time in sec. The error caused by the counting statistic was turned out to be less than 1% in the whole exposure rates determined in this study.

## 4. Results and Discussion

### 1) Background Spectrum

In order to figure out "pure" leakage gamma-rays from the spectra measured in reactor operations, background spectra were measured at each corresponding point of measurement under the identical condition under which the leakage gamma-rays were measured, except for the reactor shut down.

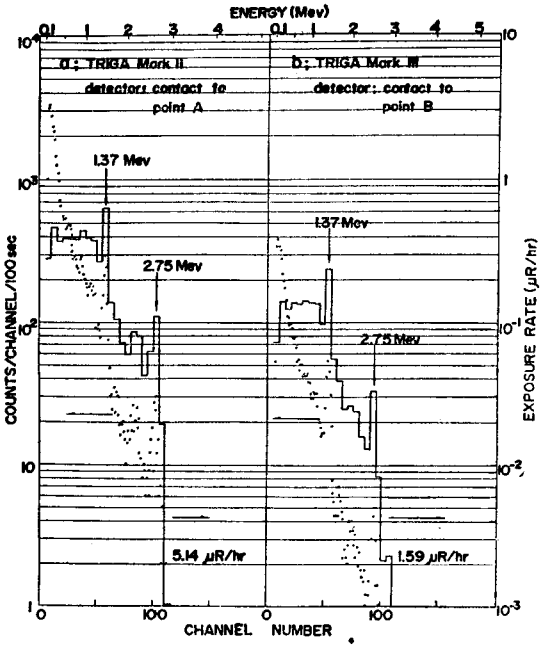


**Fig. 8. Typical background spectra at reactor wall surface**

Two typical background spectra are shown in Fig. 8. In this figure, solid circles indicate counts/channel and corresponding spectrum of exposure rate is expressed by histogram at an interval of 5 channels.

**Table 2. Background exposure rate ($X_b$) at the shielding wall surface of TRIGA Mark II**

unit; μR/hr

| Measured Position | | A | D | G |
|---|---|---|---|---|
| Distance from Wall Surface (cm) | contact | 5.14 | 25.49 | 6.21 |
| | 50 | 7.44 | 103.83 | 7.39 |
| | 100 | 8.76 | 2272.03 | 9.93 |

As shown in the figure, each spectrum shows two distinct photopeaks of 1.37MeV and 2.75 MeV in addition to ordinary background spectrum which shows a coutinuous

**Table 3. Background exposure rate($X_b$) at the shielding wall surface of reactor TRIGA Mark III**

unit; $\mu$R/hr

| Measured Position | A** | B | D* | E | F* | G | I | K | M | O | P* | Q | R* | T | vdp. | mean$\pm\sigma$ |
|---|---|---|---|---|---|---|---|---|---|---|---|---|---|---|---|---|
| $X_b$ | 0.79 | 1.59 | 2.28 | 1.58 | 1.43 | 1.80 | 1.82 | 2.04 | 1.94 | 1.84 | 1.44 | — | 1.51 | 1.67 | 1.65 | 1.67$\pm$0.34 |

*: at 15cm from the wall surface
**: at 45cm from the wall surface

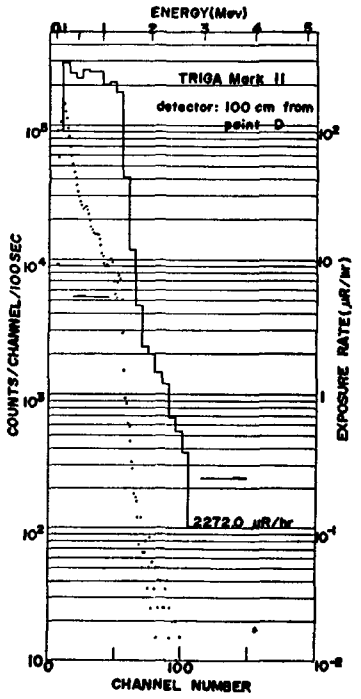


**Fig. 9. An extraordinary qckground spectra in reactor hall of TRIGA Mark II**

decrease in counts/channel from minimum detectable energy up to about 3 MeV[23-25]. The photopeaks are likely due to the contribution of gamma-rays emitted from activated $^{24}Na$ which may be involved in reactor shielding concrete. Comparing the background spectrum *a* with *b* in Fig. 8, which were measured for TRIGA Mark II and III, respectively, it is noticed that spectrum *a* shows higher count rates in each corresponding channel of the spectrum. Accordingly, the total exposure rate of *a* is also higher than that of *b*. The difference between the two typical background spectra may be attributed to either causes of; (1) a cumulative effect due to longer operating time of the former reactor[26] or (2) a contributive effect of other radiation source exists in the former reactor hall.

In fact, the second cause was identified in the reactor hall of TRIGA Mark II, that is, near the bulk shielding tank there was a resolved rotary specimen rack kept in a simple temporary shield. Thus, as shown in Fig. 9, an extremely high background spectrum was observed at point D which is the nearest to the source.

Values of the background exposure rates at the reactor shilding walls are summarized in Tables 2 and 3.

Evidence of the contributive effect to background radiation by other radiation source in the reactor hall of TRIGA Mark II is easily shown in Table 2, *i.e.*, the exposure rate of the background is increasing with distance from the reactor wall surface. On the contrary, background exposure rates measured for TRIGA Mark III are comparatively even except for the value measured at point A. At point A, there was a distance of 45cm between the reactor wall and detector, hence a reasonable attenuation of the background radiation from the reactor wall is expected. Averaged value of the background exposure rate in the case of TRIGA Mark III is 1.67$\pm$0.34$\mu$R/hr.

However high the background exposure rate and whatever the shape of the spectrum may be, it actually does not make any disturbance in leakage gamma-ray analysis as far as the energy spectrometry is applied, since the spectrum of a gamma-ray source located outside

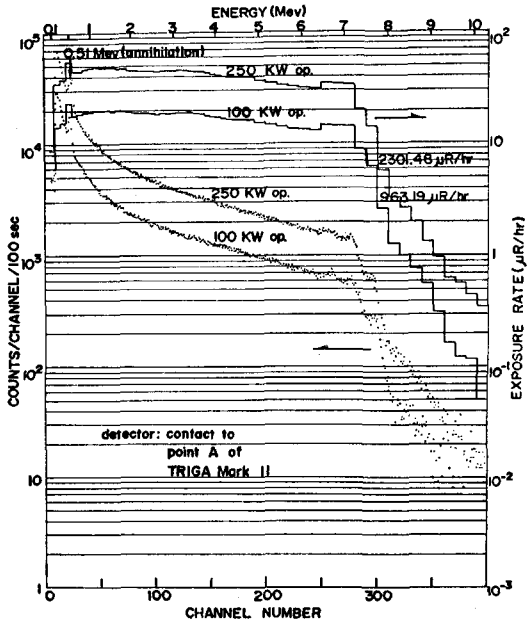


**Fig. 10. Typical spectra of reactor leakage gamma-rays (TRIGA Mark II)**

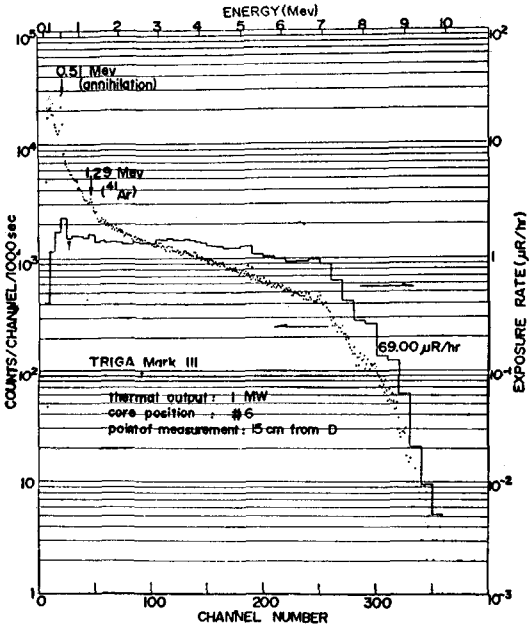


**Fig. 11. A spectrum of leakage gamma-rays out of TRIGA Mark III (1)**

the reactor should be different from that of the leakage gamma-rays. Necessity of the background spectrometry and subsequent subtracting it from each corresponding spectrum of leakage gamma-rays exists at this point.

### 2) Characteristics of Leakage Gamma-ray Spectrum

The pattern of a leakage gamma-ray spectrum is characterized by its particular energy distribution which shows a continuous and smooth distribution in counts per energy interval (channel) from 0.1 to about 7~8 MeV with an annihilation peak at 0.51 MeV, and in the range of energy higher than 8 MeV counts per channel is rapidly falling down. A typical spectrum of leakage gamma-rays observed in this study is shown in Fig. 10.

In the figure solid cireles and histogram indicate counts/channel and corresponding exposure rate, respectively. This typical spectrum of the leakage gamma-rays shows fairly good agreement in its pattern with the gamma-ray spectrum observed in in-core or fission

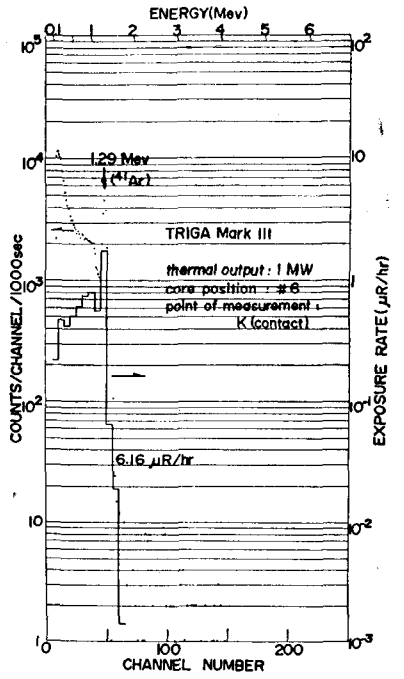


**Fig. 12. A spectrum of leakage gamma-rays out of TRIGA Mark III (2)**

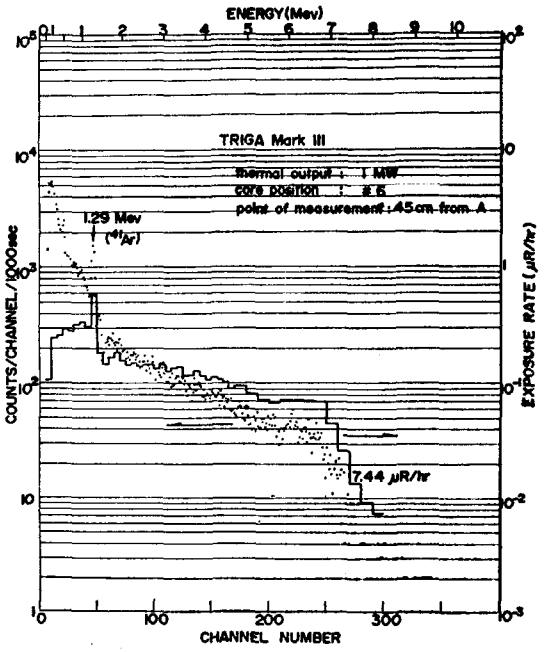


**Fig. 13. A spectrum of leakage gamma-rays out of TRIGA Mark III (3)**

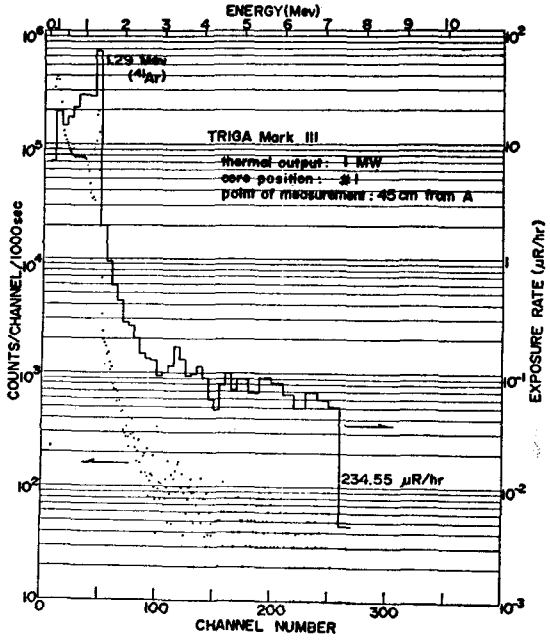


**Fig. 14. A spectrum of leakage gamma-rays out of TRIGA Mark III (4)**

spectrometry conducted by others[1, 10, 27] using pair spectrometer or Compton scattering anti-coincidence spectrometer. As it was expected, the pattern itself of the leakage gamma-ray spectrum is turned out to be essentially unaltered, although there must be a considerable attenuation in intensity through the shielding wall.

In Fig. 10 two spectra are shown, *i.e.*, spectrum of leakage gamma-rays on 100KW and 250KW operations of TRIGA Mark II, respectively.

The pattern of the spectrum are also independent of thermal output of the reactor as shown. The same pattern of the leakage gamma-ray spectrum was observed at different points of measurement in TRIGA Mark II reactor hall.

For the reactor TRIGA Mark III, however, there is a variety in pattern of the measured spectra according to operating core position

**Table 4. Leakage gamma-ray exposure rate ($\dot{X}_l$) at the wall surface of reactor TRIGA Mark II**

unit: $\mu$R/hr

| Thermal Output (KW) | Measured Point / Distance from Wall (cm) | A | D | G |
|---|---|---|---|---|
| 100 | contact | 963.19 | 696.81 | 791.52 |
| | 50 | 719.60 | 533.41 | 640.91 |
| | 100 | 563.70 | 407.62 | 506.97 |
| 250 | contact | 2301.49 | 1730.77 | 1964.93 |
| | 50 | 1760.89 | 1347.51 | 1577.25 |
| | 100 | 1395.79 | 991.80 | 1236.53 |

and points of measurement. An extreme comparison can be made between Figs. 11 and 12.

The two spectra were measured at different point for the same core position and at the same operating power of the reactor TRIGA Mark III. However, the former shows a typical

**Table 5. Leakage gamma-ray exposure rate ($\dot{X}_l$) at the wall surface of reactor TRIGA Mark III (1)**

unit: $\mu$R/hr

| Thermal Output (MW) | Core Position | Measured Point | | | | | | |
|---|---|---|---|---|---|---|---|---|
| | | A** | B | D* | E | F* | G | I |
| 1 | #6 | 7.44 | 1.36 | 69.00 | 16.13 | 75.80 | 84.09 | 8.51 |
| // | #3 | 0.32 | 0.36 | 1.00 | 0.47 | 4.34 | 62.11 | 2.20 |
| // | #1 | 234.55 | 125.79 | 194.77 | 199.47 | 166.87 | 89.12 | 396.99 |
| 2 | #6 | 43.94 | — | 561.50 | 148.73 | 217.24 | 235.24 | 20.22 |
| // | #3 | 2.20 | 4.20 | 2.28 | 3.59 | 20.46 | 308.23 | 5.64 |

*: at 15cm from the wall surface
**: at 45cm from the wall surface

**Table. 6. Leakage gamma-ray exposure rate($\dot{X}_l$) at the wall surface of reactor TRIGA Mark III (2)**

unit: $\mu$R/hr

| Thermal Output (MW) | Core Position | Measured Point | | | | | | |
|---|---|---|---|---|---|---|---|---|
| | | K | M | O | P* | R* | T | vent d. pipe |
| 1 | #6 | 6.16 | 14.21 | 1.31 | 56.01 | 56.44 | 1.62 | 2708.55 |
| // | #3 | 1.73 | 1.98 | 45.54 | 3.03 | 0.11 | 0.21 | 54.68 |
| // | #1 | 155.80 | 183.81 | 82.28 | 113.51 | — | 99.00 | 185.69 |
| 2 | #6 | 8.26 | 16.81 | 125.45 | 147.36 | — | 5.73 | 10843.11 |
| // | #3 | 2.00 | 1.11 | 111.50 | 7.69 | — | 0.83 | 118.79 |

*:at 15cm from the wall surface

leakage gamma-ray spectrum in its pattern with a small peak of 1.29 MeV, $^{41}$Ar, while the latter indcates an almost pure $^{41}$Ar spectrum without noticeable contribution of reactor leakage gamma-rays. Another comparion can also be made between Figs. 13 and 14. The two spectra were measured at the same point and at the same thermal output for different core positions. The former shows clear contribution of leakage gamma-rays in the light of distributed energy range with an eminent peak of $^{41}$Ar at 1.29 MeV, while the latter demonstrates a much hiher $^{41}$Ar peak with less contribution of the reactor leakage gammarays.

As shown through the above comparisons, measured spectra of the leakage gamma-rays for the reactor TRIGA Mark III are varied in their pattern with their points of measurement and operating core position. It is easily found that the shift in basic spectrum pattern mainly caused by contributions of radiations from other sources such as $^{41}$Ar rather than by leakage gamma-ray itself. Further discussion on the contribution of the other than leakage gamma-rays will be made later.

The values of total exposure rates calculated from each measured spectrum by the use of the conversion operator $G(E)$ are summarized in Tables 4, 5 and 6.

As shown in Table 4, the total exposure rate due to leakage gamma-rays from operating TRIGA Mark II are different according to points of measurements, but the basic pattern of the measured spectra are all the same with each other as that shown in Fig. 10. Distance

**Table 7. Gamma-ray leaking wall surface of TRIGA Mark III**

| Thermal Output (MW) | Core Position | Gamma-ray Leaking Wall |
|---|---|---|
| 1 | #6 | A, D, E, F, wall & R, P, wall |
| // | #3 | F, G, I wall & P, O wall |
| // | #1 | K, M, wall & T, P, O wall |
| 2 | #6 | A, D, E, F, I wall & T, P wall |
| // | #3 | E, F, G, I wall & P, O wall |

**Table 8. Relative attenuation of leakage gamma-ray exposure in air with distance from reactor wall surface (TRIGA Mark II)**

| Thermal Output (KW) | 100 | | | 200 | | | average |
|---|---|---|---|---|---|---|---|
| Measured Point / Distance from Wall(cm) | A | D | G | A | D | G | |
| contact | 1.000 | 1.000 | 1.000 | 1.000 | 1.000 | 1.000 | 1.000±0.000 |
| 50 | 0.747 | 0.766 | 0.810 | 0.765 | 0.779 | 0.803 | 0.778±0.022 |
| 100 | 0.585 | 0.585 | 0.641 | 0.606 | 0.573 | 0.629 | 0.603±0.025 |

resulting $\dot{X}=\dot{X}_0 \exp(-\mu D)$ where $\mu=5.06\times10^{-3}cm^{-1}$ within ±5% in the region of D≤100cm. Estimated uncertainty in $\mu$ is less than ±1%.

effect of total exposure rate of leakage gamma-rays will be examined in the next section.

The values in Tables 5 and 6 indicate the exposure rates of leakage gamma-rays measured for operating TRIGA Mark III. It should be noted, however, that those values given in the Tables may include radiations from other sources such as $^{41}Ar$ in addition to "real" leakage gamma-rays from the reactor. For instance, a comparison between the values measured for core position #6 at 1MW thermal output and those for core position #1 at the same operating power indicates a great difference in their total exposure rates at the same points of measurement. This difference in exposure rates is not necessarily due to the difference in the intensity of the leakage gamma-rays as will be shown later.

Taking those contributions of other radiations into account, and according to the careful examination on each spectrum pattern, for TRIGA Mark III, the reactor wall surfaces from which in-core gamma-rays are leaking

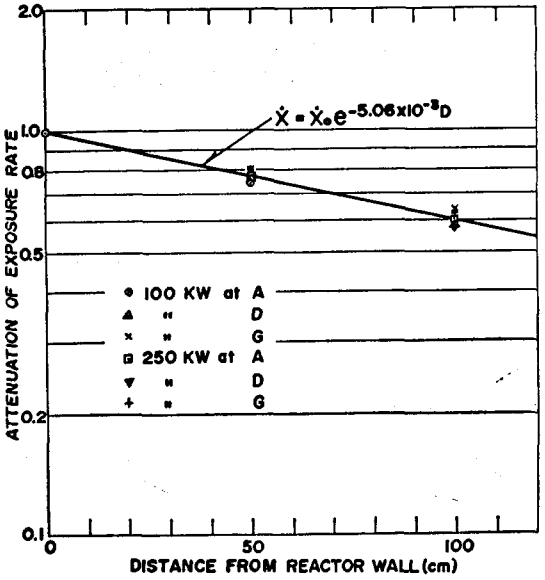


**Fig. 15. Attenuation of total exposure rate due to reactor leakage gamma-rays in air with distance from the reactor wall surface (TRIGA Mark II)**

are identified as Table 7 along with the thermal output and the operating core positions. The surfaces are indicated with alphabetic symbols showed in Fig. 4.

**3) Effects of Distance and Thermal**

**Output**

For the leakage gamma-rays from the reactor TRIGA Mark II, which are thought to be considerably free from other radiations, the distance effect on total exposure rates was investigated in the region of 1 m distance from the reactor wall. This region of the distance is the place where personnel are most frequently staying at work.

Table 8 shows the relative attenuation of the total exposure rate due to the leakage gamma-rays in air with distance from the reactor wall surface. Nevertheless, changes in the basic pattern of the energy spectrum were not observed.

Relative attenuation of the total exposure rate is illustrated in Fig. 15, and from this figure it is deduced that the attenuation in air follows a simple exponential law with an attenuation coeffcient of $5.06\times10^{-3}cm^{-1}$, that is

$$\dot{X}=\dot{X}_0e^{-5.06\times10^{-3}D}.$$

**Table 9. $\dot{X}_{250}/\dot{X}_{100}$ ratio for TRIGA Mark II leakage gamma-rays**

| Measured Point / Distance from wall(cm) | A | D | G | average |
|---|---|---|---|---|
| contact | 2.39 | 2.48 | 2.48 | 2.45 |
| 50 | 2.45 | 2.53 | 2.46 | 2.48 |
| 100 | 2.48 | 2.43 | 2.44 | 2.45 |
| average | 2.44 | 2.48 | 2.46 | 2.46 |

Here, $\dot{X}_0$ : total leakage gamma-ray exposure rate at the reactor wall surface

$\dot{X}$ : total leakage gamma-ray exposure rate at D cm from the reactor wall surface.

According to the fitting the values given in Table 8 to the cuve given by the exponential equation, the total exposure rate due to reactor leakage gamma-rays in a certain region of distance concerned is well predicted within an accuracy of ±5%. Estimated uncertainty in the attenuation coefficient is less than 1%. With this exponential law, the exposure rates measured at places distant from the reactor wall surface of the TRIGA Mark III(refer to Tables 1, 5 and 6) can be corrected, if necessary, to those values at the wall surfaces.

The effect of reactor thermal output ongammarays was also examined. Table 9 shows the effect numerically.

$\dot{X}_{250}$ indicates the total leakage gamma-ray exposure rate at a certain point of measurement on 250KW operation and $\dot{X}_{100}$ is that at the identical point on 100KW operation. As shown in the Table, the total exposure rate due to the reactor leakage gamma-rays is nearly proportional to the thermal output of the reactor without changing the basic spectrum pattern.

**4) Other Gamma-rays Originating in Reactor Operation**

As mentioned earlier, the leakage gamma-ray spectra and the total exposure rates measured in the reactor TRIGA Mark III are a complex function of field geometry, core position and

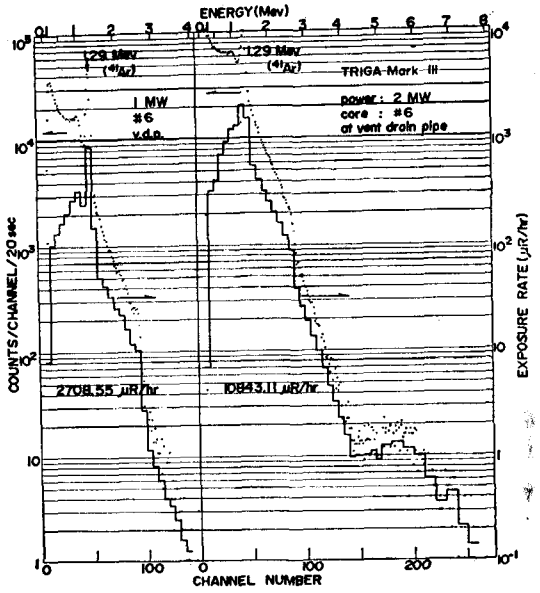


**Fig. 16. Gamma-ray spectrum measured at surface of vent drain pipe of TRIGA Mark III**

reactor power. Such a phenomenon was not observed in the case of TRIGA Mark II which is a simple fixed-core, pool type reactor. It is, however, easy to say, with a help of spectrum analysis, that those complexity observed in TRIGA Mark III are not caused by the leakage gamma-ray alone.

Reviewing Tables 5 and 6, it is noticed that the whole values of total exposure rates are very high in the case of operating core position #1, and extraodinarily high values appered at vent drain pipe when the core is located at position #6. Fig. 16 shows the measured spectra at surface of the vent drain pipe with core position #6. As shown in the figures, the spectra indicate gamma-rays of energy much lower than that of leakage gamma-rays with a prominent photopeak of 1.29MeV, $^{41}$Ar gamma-ray.

Accoding to these spectra, the gamma-rays being emitted from the pipe are due to the activated air dust being removed through the pipe from the reactor beam ports. Neutron activations of air will produce radioisotopes of nitrogen, exygen, argon, the rare gases in air, and possibly carbon oxide[28-30]. All these are fairly short lived with the excepton of the $^{41}$Ar whose half life is 1.83 hours. Actually on the right hand side spectrum of Fig. 16, which was measured 2MW thermal output, weak contribution of $^{16}$N is noticed near 6MeV region.

Particularly remarkable contribution of $^{41}$Ar is observed in whole the spectra measured for core position #1 where a large biological irradiation cell is directly contacted to the operating reactor core. Diffusion of the activated $^{41}$Ar in the reactor hall through the slit of the shielding door of the irradiation cell (refer to point M in Fig. 4) raises whole the exposure rate in the reactor hall. As an example let us review the spectrum measured at point A when the core is located at position #1. As found in Fig. 14 and Table 5, the total exposure rate at this point is about 234$\mu$R/hr. Normalizing the spectrum of Fig. 14 to the spectrum measured at the same point with core position #6 (Fig. 13), at high energy region of the spectrum which is mainly constituted of leakage gamma-rays, the Fig. 14 can be

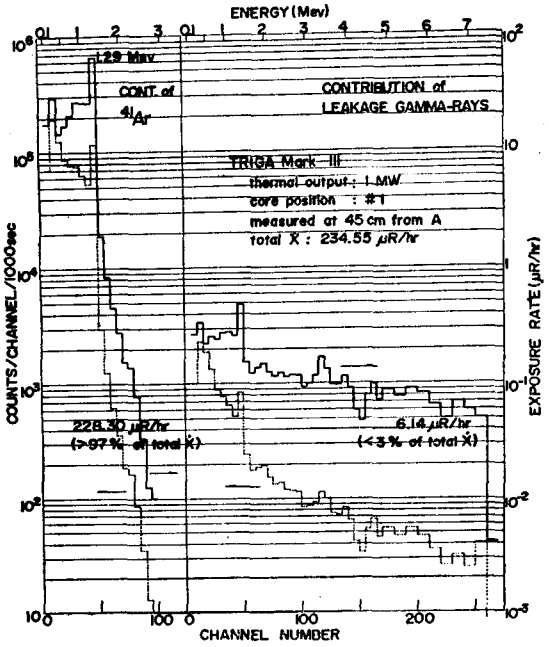


**Fig. 17. A spectrum resolution to show the contribution of $^{41}$Ar and "pure" leakage gamma-rays to total exposure rate (TRIGA Mark III)**

resolved into two parts, *i.e.*, the spectrum due to $^{41}$Ar and that due to reactor leakage gamma-rays.

Fig. 17 shows the two resolved spectra. In the figure counts/channel are averaged at an interval of 5 channels and indicated by dotted histogram, and corresponding exposure rates are indicated by soild histogram. As this figure shows, more than 97% of the total exposure rate at this point under the specified condition is contributed by the gamma-rays emitted by $^{41}$Ar, and accordingly the contribution of reactor leakage gamm-rays is less than 3% of the total exposure rate. Uncertainty involved in this spectrum resolution is less than 0.05%

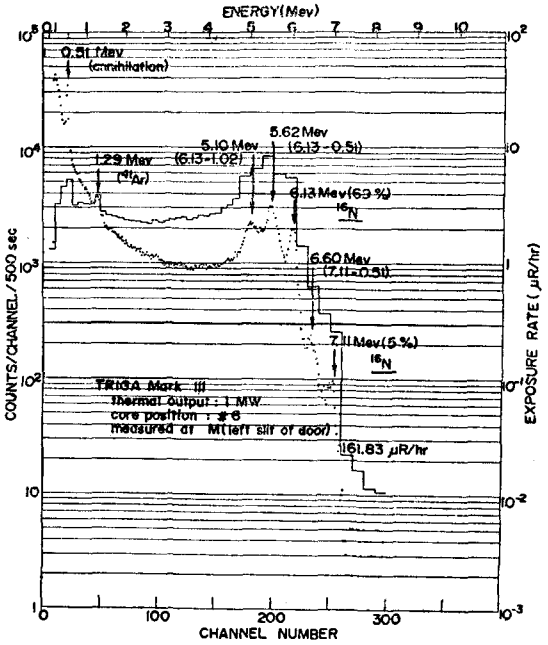


**Fig. 18. A spectrum showing origination of $^{16}N$ in biological irradiation room of TRIGA Mark III during the course of reactor operation**

of the total exposure rate which is negligible enough. Stable isotope of argon, $^{40}Ar$, is known to comprise about 1% of normal air, and since argon is an inert gas the greater concern on activated $^{41}Ar$ is not the internal dose, but is the external dose[29].

Further, diffusion of the activated $^{16}N$ near the shield door of irradiation cell was observed. Fig. 18 shows a spectrum measured at the left side slit of the shield door with the reactor core operated at position #6, the farthest core position from the irradiation cell. This gamma-ray spectrum, however, exhibits clearly the leakage of gaseous $^{16}N$ from the biological irradiation cell. $^{16}N$ emits 69% of 6.13 MeV photons and 5% of 7.11MeV photons per nuclear decay. Fig. 18 shows 6.13MeV and 7.11MeV photopeaks with single escape peaks of 6.60 (=7.11−0.51)MeV, 5.62(=6.13−0.51) MeV, and 5.10(=6.13−1.02) MeV double escape peak in addition to 0.51MeV annihilation peak and 1.29 MeV photopeak of $^{41}Ar$. Such a production of $^{16}N$ is attributable to the(n, p) reaction on $^{16}O$ in the air of the irradiation cell[31]. Because of its short half-life (7 sec), $^{16}N$ was not noticed at other points of measurement, but at point M which is the nearest point to the slit of the shield door, it was always observed although there were some differences in detected amount depending on the operating core position.

## 5. Conclusions

The importance of the dosimetrical analysis of the reactor leakage gamma-rays was thoroughly mentioned before. Of the means of dosimetrical analysis, the scintillattion spectrometry is turned out to have such strong advantages as; i) that enables to distinguish the "real" leakage gamma-rays from gamma-rays emitted by other soueces, ii) because of the inherent high sensitivity of NaI(Tl) scintillator for detecting photons, exposure rates due to the leakage gamma-rays quantifield at the level as low as an order of $\mu$R/hr with fairly good accuracy. Thus, the application of scintillation spectrometry in dosimetrical analysis of reactor leakage gamma-rays is fully justifield.

The conclusions derived through this investigation are as follows;

(1) In the energy region of the reactor leakage gamma-rays, Moriuchi's spectrum-exposure rate conversion operation is one of the most effective method as far as scintillation spectrometry is applied to determine the total exposure rates due to the "real" leakage gamma-rays with satisfactory accuracy in health physics point of view, particularly when a large number of spectra are to be converted into exposure rates.

(2) The basic pattern of the "typical" spectrum of the reactor leakage gamma-rays is neither affected by thermal output of the reactor, nor influenced by overall attenuation.

This enables us to stripping out the component of gamma-rays contributed by other sources from a cmplex spectrum involving reactor leakage gamma-rays by normalizing it to the basic pattern of the leakage gamma-ray spectrum.

(3) The attenuation of the leakage gamma-rays, in air, in terms of exposure rate as a whole follows a simple exponential law with an attenutaion coefficent of $5.06\times10^{-3}cm^{-1}$, irrespective of the spectrum covering a wide range of photon energies. The total exposure rate due to the leakage gamma-rays at a certain point is nearly proportional to the thermal output of the reactor.

(4) In the case of a pool-type reactor of movable core with a large self-contained irradiation cell, like TRIGA Mark III, the pattern of the measured gamma-ray spectrum is a complex function of place of measurement, operating core position and thermal output of the reactor, regardless of the corresponding total exposure rate.

(5) Therefore, cluse of leakage gamma-rays from a reactor should be traced by the energy distribution of the detected photons which normally ranges up to 7 MeV or higher, rather than simply by the total exposure rate measured, since gamma-rays from other sources such as $^{41}Ar$ or $^{16}N$ originating during the course of reactor operation may contribute to raise the total exposure rates even if the leakage gamma-rays are actually negligible.

## Acknowledgements

The author is gratefully indepted to Dr. Chaeshik Rho of KAERI for his warmhearted encouragements to carry out this work, and wishes to thank Mr. Seung Gy Ro of the Institute for many valuable disussions with reviewing this manuscript. Thanks are also due to Miss He Hwa Im of Dept. of Physics, Sookmyung Women's University for her kind assistance in calculating and analyzing the relevent data.

## References

1) F. Maienschein and T. Love; Nucleonics **12** (5), 7 (1954)
2) F. C. Maienschein *et al.*; Proc, 2nd Int. Conf. PUAE, Vol. 15, PP. 366-372, Geneva (1958)
3) R. W. Peelle and F. C. Maienschein; Nucl. Sci. Eng. **40**, 485 (1970)
4) G. T. Champman and W. R. Burrus; Nucl. Sci. Eng. **34**, 169 (1968)
5) V. Kadlec; in I. A. E. A Tech. Rept. No. 127, PP. 37-83, IAEA, Vienna (1971)
6) Y. Nakashima *et al*; J. Japan Atom. Energ. Soc. **12**, 577 (1970)
7) S. Moriuchi and I. Miyanage; Health Phys. **12**, 541 (1966)
8) I. Miyanaga and S. Moriuchi; J. Japan Atom. Energ. Soc. **9**, 440 (1967)
9) S. Moriuchi; JAERI-1209 (1971)
10) V. V Verbinski *et al.*; Phys. Rev. C **7**, 1173 (1973)
11) A. Ono; Nucl. Eng. **18**(7), 32 (1972)
12) D. Engelkemeir; Rev. Sci. Instr. **27**, 589 (1956)
13) J. H. Hubbell; Rev. Sci. Instr. **29**, 65 (1958)
14) I. H. Hubbel and N. E. Scofield; IRE Trans. Nucl. Sci. NS-**5**, 156 (1958)
15) K. Ishimatsu; J. Japan Atom. Energ. Soc. **4**, 24 (1962)
16) S. Minato and M. Kawano; J. Nucl. Sci. Tech. **7**, 401 (1970)
17) H. Cember; Introduction to Health Physics, PP. 158-164, Pergamon Press, London (1969)
18) W. F. Miller and W. J. Show; Nucleonics **19**(11) 174 (1961)
19) R. D. Evans; in Radiation Dosimetry, Vol I (Attix and Roesch ed.), P. 93, Academic Press, London (1967)
20) ICRU Report 19, Radiation Quantities and Units, ICRU (1971)
21) Y. Moriuchi; Nucl. Eng. **15**(10), 29 (1969)
22) C. D. Zerby and H. S. Moran; ORNL-3169 (1962)
23) T. Doke *et al.*; J. Japan Atom. Energ. Soc. **1**, 53 (1959)

24) P. F. Gustafson *et al.*; Science **145**, 44 (1964)
25) S. C Bushong; Health Phys. **10**, 731 (1964)
26) T. V Anderson *et al.*; T-739, TRIGA Owner's Conference Papers and Abstracts, PP. 1-18, GEES, San Diego (1972)
27) R. W Peelle and F. C. Mainschein; ORNL-4457 (1970)
28) C. F. Stolzenbach; Nucl. Safety **6**, 433 (1965)
29) H. J. Moe *et al*; ANL-7291 (1966)
30) W. L. Smith; T-743, TRIGA Owner's Conference Papers and Abstracts, PP. 2-3 GEES San Diego (1972)
31) W. M. Lowder *et al.*; Trans. Am. Nucl. Soc **15** (1), 540 (1972)